Supporting Information

Surfactant-Free Microemulsion Composed of Isopentyl Acetate, *n*-Propanol, and Water

Yuan Liu [a], Jie Xu * [a], Huanhuan Deng [a], Jiaxin Song [a], Wanguo Hou * [b]
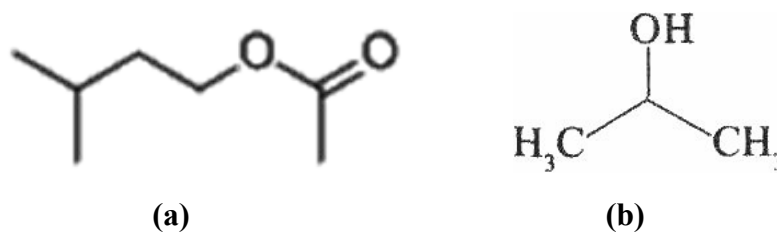
(a)   (b)

Fig. S1. Molecular structures of (a) isopentyl acetate and (b) *n*-propanol.

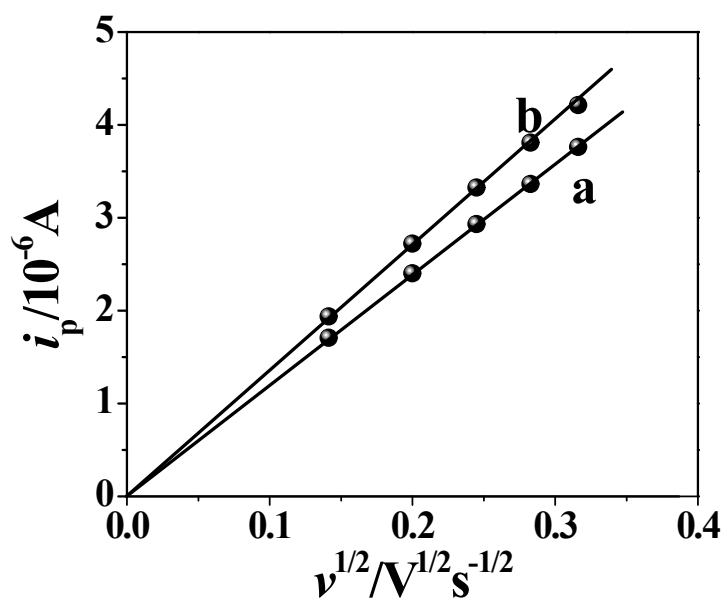**Fig. S2.** Scan-rate dependence of anodic peak currents in microemulsions at $f_{IA}=0.050$ with (a) $R_{P/W} = 8.0/2.0$ and (b) $R_{P/W} = 7.0/3.0$.
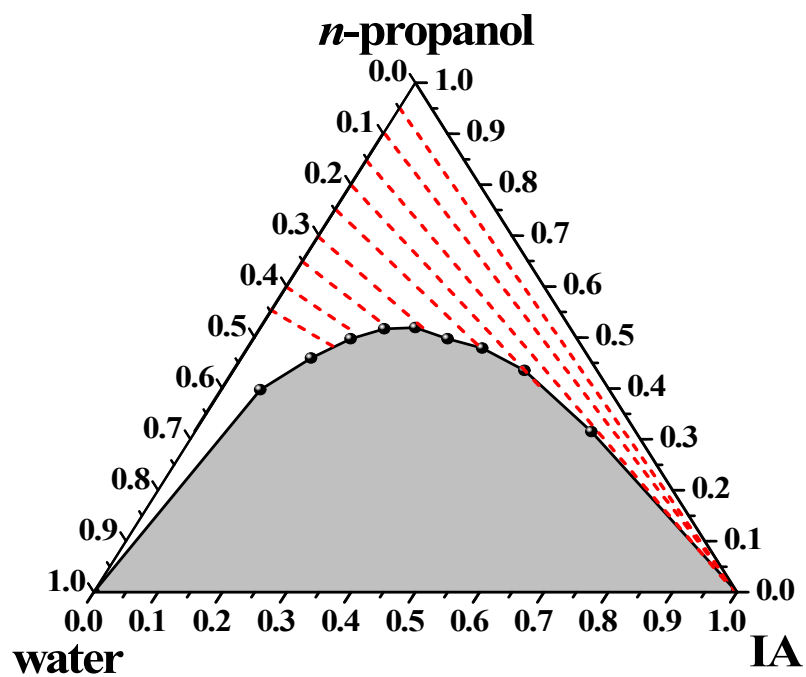
Fig. S3. IA dilution lines with different $R_{P/W}$ values for cyclic voltammetry, fluorescence spectroscopy, and UV-visible spectroscopy mesurements
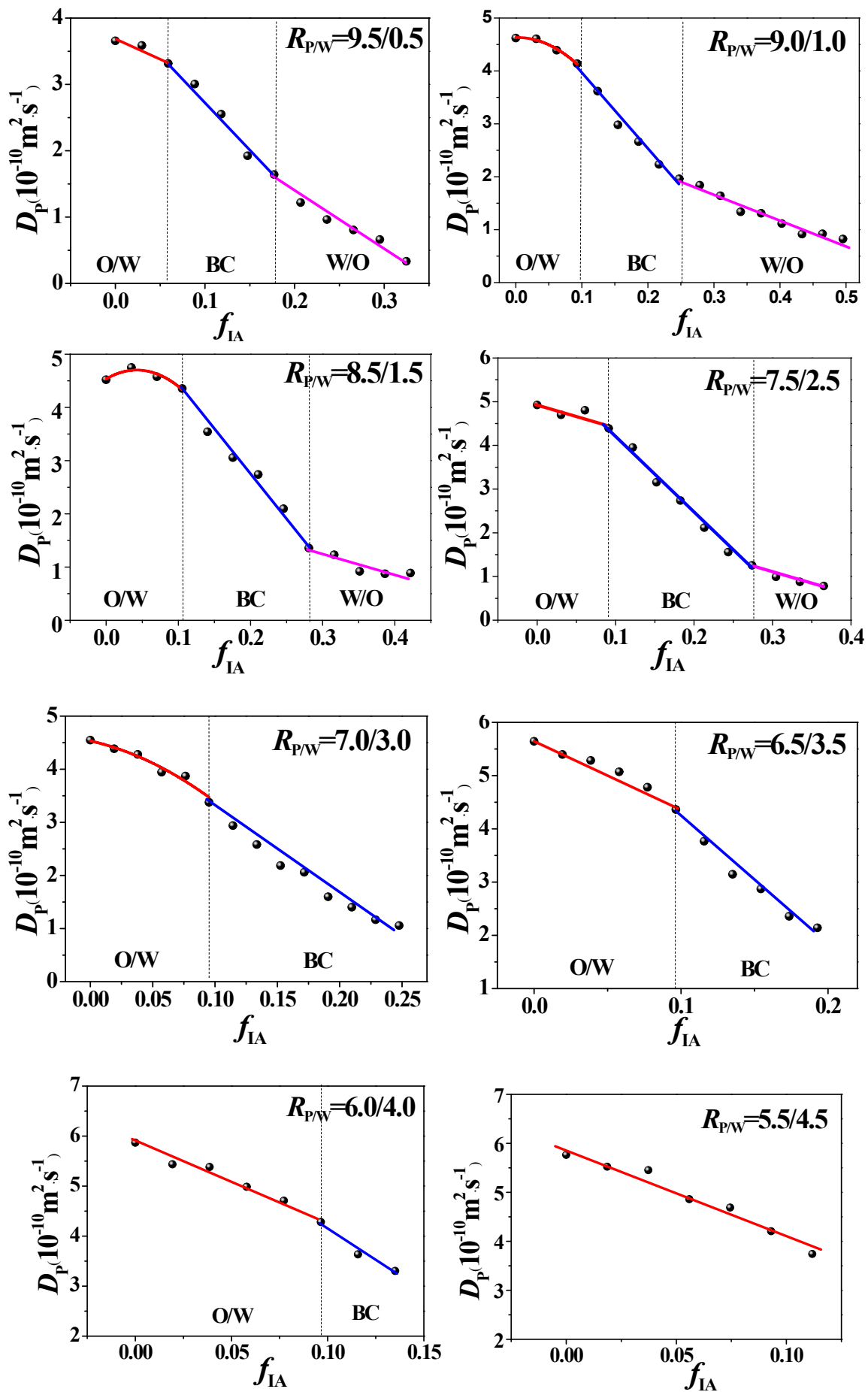
Fig. S4. Diffusion coefficient (D_p) of $K_3Fe(CN)_6$, in microemulsions as a function of f_{IA} at various $R_{P/W}$. The concentration of $K_3Fe(CN)_6$ was 0.65 g·L^{-1}.
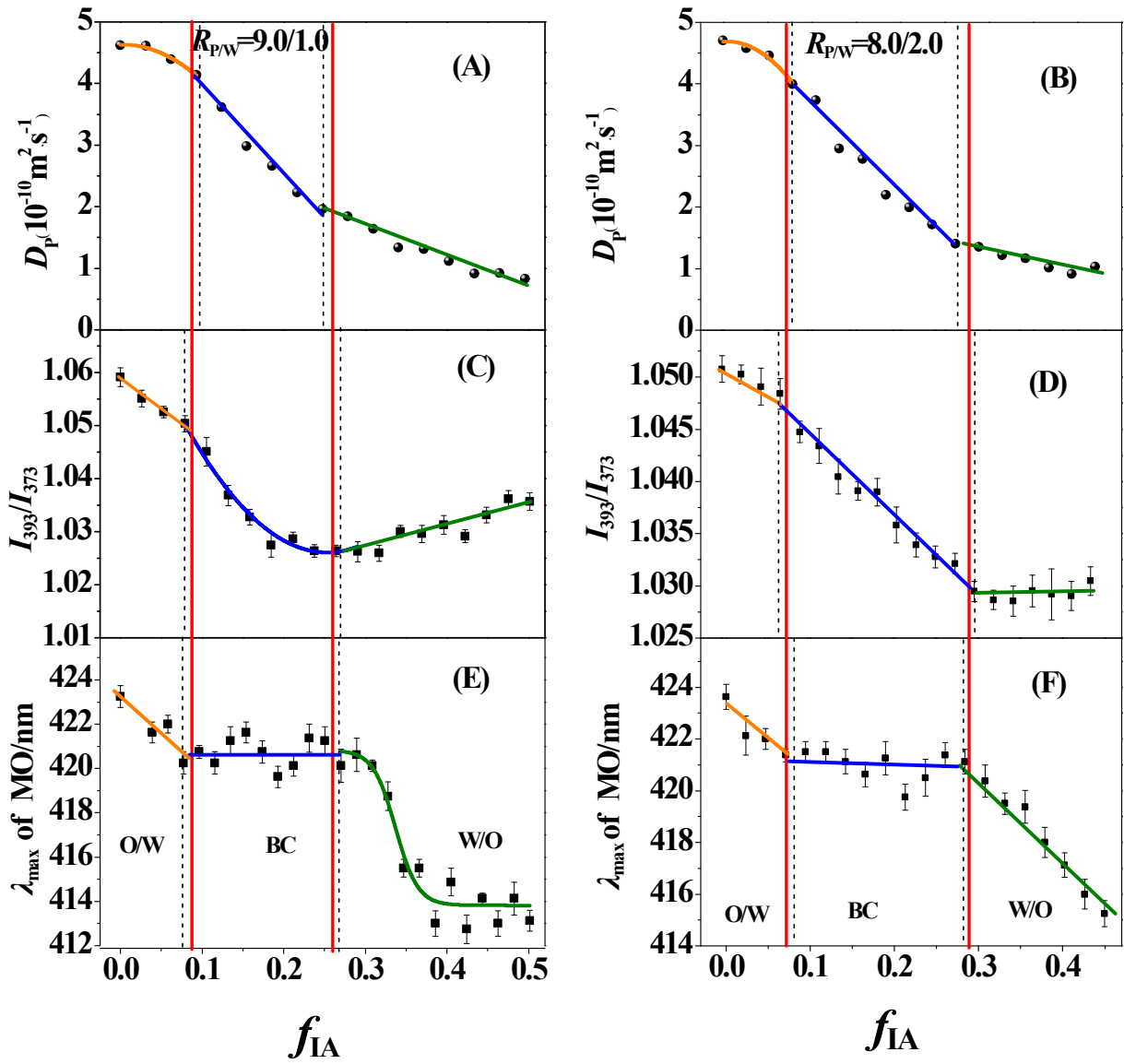
Fig. S5. (A, B) D_p of K$_3$Fe(CN)$_6$, (C, D) I_{393}/I_{373} of pyrene, and (E, F) λ_{max} of MO in microemulsions at (A, C, E) $R_{P/W}$ = 9/1 and (B, D, F) $R_{P/W}$ = 8.0/2.0 as a function of f_{IA}.
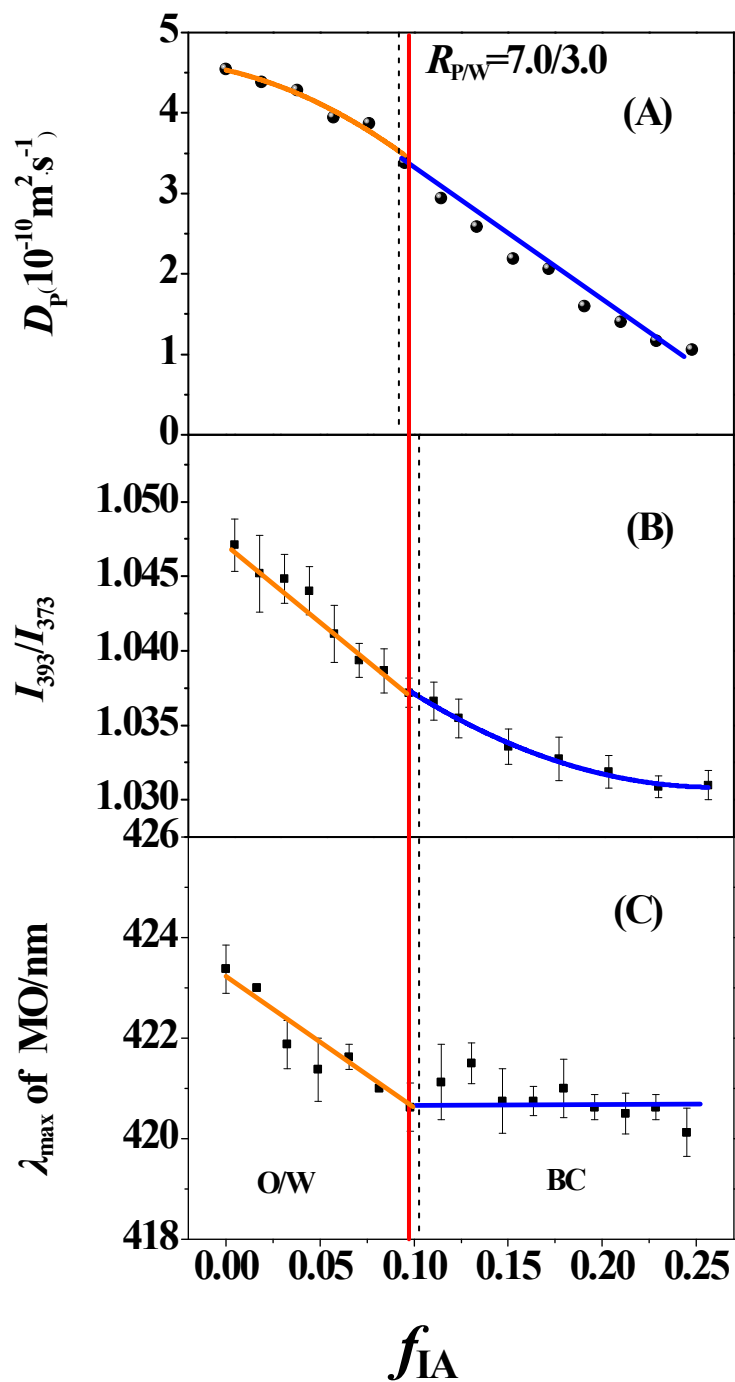
Fig. S6. (A) D_p of $K_3Fe(CN)_6$, (B) I_{393}/I_{373} of pyrene, and (C) λ_{max} of MO in microemulsions at $R_{P/W} = 7.0/3.0$ as a function of f_{IA}.
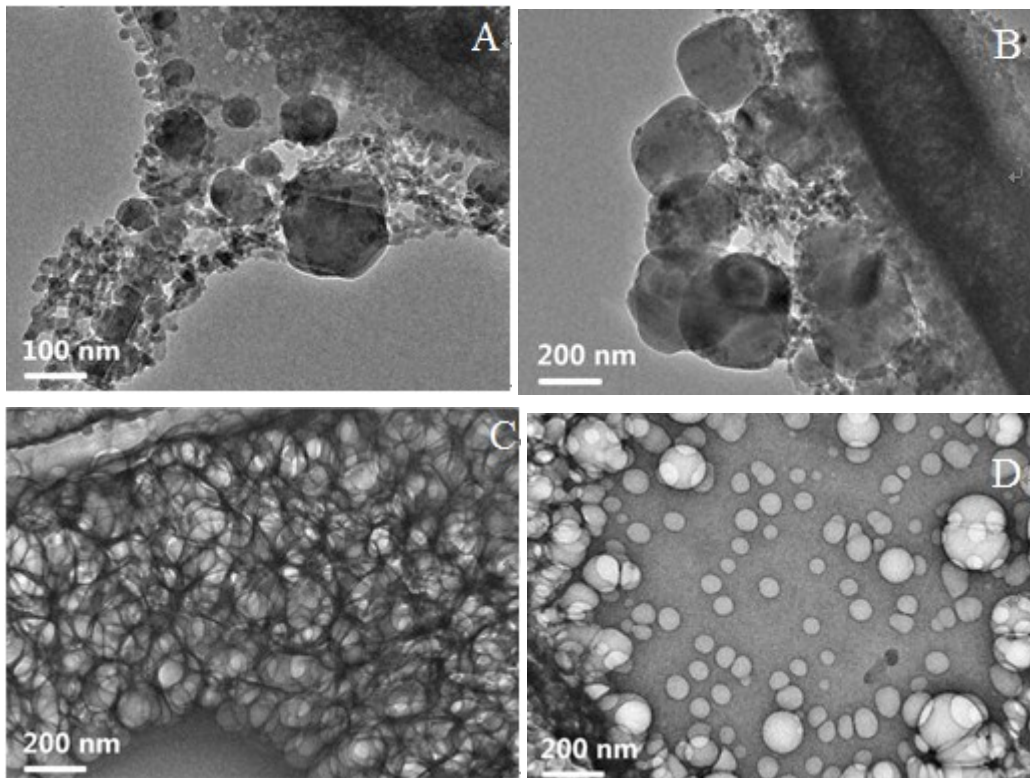
Fig. S7. Cryo-TEM images of samples (A) *a*, (B) *b*, (C) *c*, and (D) *d*. The samples *a* and *b* fall in the O/W subregion, and the samples *c* and *d* fall in the BC and W/O subregions, respectively, as marked in Fig. 1.